Isı Bilimi ve Tekniği Dergisi, 40, 2, 335-347, 2020
J. of Thermal Science and Technology

ISSN 1300-3615
https://doi.org/10.47480/isibted.817063

THERMODYNAMIC AND ECONOMIC ANALYSIS OF GEOTHERMAL ENERGY POWERED KALINA CYCLE

Merve SENTURK ACAR*
*Mechanical Engineering Dept., Engineering Faculty, Bilecik Seyh Edebali University,11230 Bilecik, Turkey,
merve.senturkacar@bilecik.edu.tr, ORCID: 0000-0003-1442-4560

(Geliş Tarihi: 19.03.2020, Kabul Tarihi: 08.10.2020)

Abstract: In this study, thermodynamic and economic analysis have been carried out to the determination of optimum design parameters of Kalina Cycle. The optimization of four key parameters (turbine inlet pressure, geothermal water outlet temperature at evaporator, condenser pressure and ammonia mass fraction) is also conducted. The thermodynamic properties of the medium temperature geothermal resource in the Simav region are used in the system designs. The energy efficiency and exergy efficiency of the system are evaluated through the thermodynamic analysis. Also, the system has been investigated economically with the net present value method. As a result of the exergy analysis, it is determined that the maximum exergy destruction occurs in the evaporator within the total exergy destruction of the system. In the system design with 90 % ammonia mass fraction, the exergy destruction in the evaporator constitutes 66.5 % of the total exergy destruction in the system. The geothermal water outlet temperature at evaporator, ammonia mass fraction, turbine inlet pressure and condenser pressure of the most effective geothermal energy powered Kalina Cycle are determined as 353.15 K, 90 %, 4808 kPa and 700 kPa, respectively. The energy efficiency and exergy efficiency of this system are calculated as 13.04 % and 51.81 %, respectively. Also, the net present value of this system is calculated as 119.377 Million US$ and it is seen that it is suitable for investment in economic terms.
Keywords: Kalina cycle, Geothermal energy, Net present value, Energy, Exergy.

JEOTERMAL ENERJİ KAYNAKLI KALİNA ÇEVRİMİNİN TERMODİNAMİK VE EKONOMİK ANALİZİ

Özet: Bu çalışmada, jeotermal enerjiyle çalışan Kalina Çevrimi'nin optimum tasarım parametrelerinin belirlenmesi için termodinamik ve ekonomik analizler yapılmıştır. Türbin giriş basıncı, evaporatördeki jeotermal akışkan çıkış sıcaklığı, kondanser basıncı ve amonyak kütle oranı sistemin değişken parametreleridir. Simav bölgesindeki orta sıcaklıklı jeotermal kaynağın termodinamik özellikleri sistem tasarımlarında kullanılmıştır. Sistemin enerji ve ekserji verimleri termodinamik analizler ile değerlendirilmiştir. Ayrıca, sistem net bugünkü değer yöntemi ile ekonomik olarak incelenmiştir. Ekserji analizi sonucunda, sistemin toplam ekserji yıkımı içerisinde maksimum ekserji yıkımının evaporatörde meydana geldiği tespit edilmiştir. Kütlece % 90 amonyak bileşenli sistem tasarımında, evaporatördeki ekserji yıkımı, sistemdeki toplam ekserji yıkımının % 66.5'ini oluşturmaktadır.Ekserji analizleri sonucunde en yüksek ekserji yıkımının evaporatörde oluştuğu ve % 90 amonyak bileşenli sistem tasarımında, evaporatördeki ekserji yıkımı, toplam sistemdeki ekserji yıkımının % 66.5'ini oluşturmaktadır. En etkin sistem tasarımının enerji verimliliği ve ekserji verimliliği sırasıyla % 13.04 ve % 51.81 olarak belirlenmiştir. Optimum sisteme ait evaporatördeki jeotermal su çıkış sıcaklığı, amonyak kütle oranı, türbin giriş basıncı ve kondenser basıncı sırasıyla 353.15 K, % 90, 4808 kPa ve 700 kPa olarak belirlenmiştir. Bu sisteme ait enerji verimliliği ve ekserji verimliliği sırasıyla % 13.04 ve % 51.81 olarak belirlenmiştir. Ayrıca bu sistemin net bugünkü değeri 119.377 Milyon ABD$ olarak hesaplanmış ve ekonomik açıdan yatırıma uygun olduğu görülmüştür.
Keywords: Kalina çevrimi, Jeotermal enerji, Net bugünkü değer, Enerji, Ekserji.

NOMENCLATURE

C	Cost [$]
c	Specific heat [$kJ/\ kg\cdot K$]
D_{tube}	Diameter of the inlet pipe [m]
e^0	Molar exergy [kJ/mol]
$\dot{Ex}$	Exergy [kW]
F	Cost Factor
h	Specific enthalpy [kJ/kg]
$\dot{m}$	Mass flow [kg/s]
M	Molar mass [kg/mol]
NPV	Net present value
$\dot{Q}$	Heat energy [kW]
Q_{vs}	Volume flow rate of separator [m^3/s]
T	Temperature [K]
U	Heat transfer coefficient [$W/m^2\cdot K$]

u_t	Terminal velocity of separator [m/ s]
V	Total volume of separator [m^3]
$\dot{W}$	Power [kW]
ρ	Density [m^3/ kg]
ε	Exergy efficiency [%]
α	Ammonia mass fraction [%]
ψ	Specific exergy [kJ/kg]
η	Energy efficiency [%]

Subscripts

b	Benefit
BM	Bare module
c	Condenser
ch	Chemical
cw	Cooling water
elec	Electricity
eva	Evaporator
g	Generator
gf	Geothermal fluid
i	Interest rate
ic	Investment cost
j	Discount rate
l	Liquid
M	Material
m,i	Inlet mass flow
m,o	Outlet mass flow
moc	Maintenance and operating
ol	Life time of system
ncf	Net cash flow
p	Pump
P	Pressure
ph	Physical
r	Recuperator
sc	Salvage cost
sep	Separator
sys	System
v	Vapor
wf	Working fluid
t	Time (year)
tr	Turbine
0	Dead state

Abbreviations

CEPCI	Chemical Engineering Plant Cost Index
GEPKC	Geothermal Energy Powered Kalina Cycle
OFC	Organic Flash Cycle
ORC	Organic Rankine Cycle

INTRODUCTION

Due to the increase in energy demand and the decrease in fossil fuel reserves and pollution of the environment, research on power generation from renewable energy sources and increasing the energy efficiency of these systems gained importance (Arslan, 2010; Arslan, 2011; Deepak et al., 2014; Yari et al., 2015; Zare and Moalemian, 2017; Acar and Arslan, 2019). Geothermal energy is one of the most preferred renewable energy sources in terms of sustainability. It is also important because of the absence of environmental pollutants in the Kalina cycle due to the re-injection of geothermal fluid. Also, developing countries tend to use renewable energy sources to ensure energy diversity and energy security. Kalina Cycle (KC) is one of the low-temperature power cycles in which is using ammonia and water mixture as working fluid (Arslan, 2010; Arslan, 2011; Kalina, 1984; Saffari et al., 2016; Igobo and Davies, 2016).

In literature, different configurations of KC and operating parameters of cycles were investigated according to the thermodynamic and economic analysis. In the studies on KC, the ammonia mass fraction of ammonia-water mixture was changed between 50-90 % (Singh and Kaushik, 2013; Modi and Haglind, 2015; Sadeghi et al., 2015). Arslan (2010) investigated optimum geothermal water outlet temperature at evaporator and ammonia mass fraction of Kalina cycle system (KCS-34) according to the exergoeconomic analysis. The results show that energy efficiency of 14.9 % and exergy efficiency of 36.2 % can be achieved for optimum system design with an ammonia mass fraction of 90 %. Arslan (2011) used artificial neural network for optimization of geothermal energy powered KC and determined that the optimum ammonia mass fraction ranges from 80 % to 90 % for KCS-34. Sun et al. (2014) investigated the performance and optimum parameters of solar driven KC. They determined that the maximum annual power generation of system was 553520 kWh and the energy and exergy efficiencies of the system were 6.48 % and 35.6 %, respectively. Zare and Ashouri et al. (2015) compared the performance of fuel and solar powered KC. They found that the levelized cost of electricity of solar KC higher than fuel driven KC. Yari et al. (2015) compared the low-grade heat source powered trilateral Rankine Cycle, Organic Rankine Cycle (ORC) and KC from the viewpoint of exergoeconomic. Moalemian (2017) analyzed the parabolic solar collector integrated KC in the point view of energy, exergy and economic analysis. Saffari et al. (2016) used artificial bee colony algorithm according to thermodynamical analysis of Husavik power plant to determine the optimum operating conditions of KC. The optimum value of exergy and thermal efficiencies were determined as 20.26 % and 48.18 %, respectively.

Wang and Yu (2016) investigated the performance of a composition-adjustable KC. They indicated that the thermal efficiency of the composition-adjustable KC higher than conventional KC. Wang et al. (2017) investigated the efficiency improvement of a KC by sliding condensation pressure theoretically and numerically. They mentioned that the condenser pressure has significant effects on the system performance. The maximum energy and exergy efficiencies of the optimum design were determined as 10.48 % and 48.10 %, respectively. Rodríguez et al. (2013) compared the geothermal energy powered ORC and KC according to thermodynamical and economic analysis. They mentioned that R-290 for ORC and the ammonia-water mixture with 84 % ammonia mass fraction for KC are the most effective working fluids in the point view of

economic analysis. Varma and Srinivas (2017) compared the performance of ORC, Organic flash cycle (OFC) and KC for low temperature heat recovery. They stated that OFC had been generated maximum power. Zhang et al. (2012) indicated that KC more effective than ORC in the point view of thermodynamic analysis in their review research. Li et al. (2013) compared the performance of KC and e- KC in which the ejector was replaced with the throttle valve. They mentioned that the e - KC more effective than KC. Eller et al. (2017) analyzed the pressure, heat exchanger capacity and power output of ORC and KC for 473.25 K, 573.25 K and 473.25 K heat source temperature. They mentioned that the grassroot cost of ammonia-water KC was the lowest in the investigated source temperature range. The grassroot costs of KC were changed between 1203.4 €/kW and 619.4 €/kW. Cao et al. (2018) optimized the Kalina-Flash cycles by genetic algorithm. They determined that the Kalina -Flash cycles more effective than KC from thermodynamic and economic point of view. Nasruddin et al. (2009) reported that the optimum ammonia mass fraction was 78 % for geothermal powered KC according to thermodynamical analysis. Mergner and Weimer (2015) mentioned that the KSG-1 was more effective than the KCS-34 for geothermal power generation. He et al. (2014) investigated the performance of two modified KCS-11 cycle and KCS-11. Also, they determined the effects of two different key parameters (ammonia mass fraction and cooling water temperature) on the performance of the systems. The energy efficiency, power output and exergy efficiency of the systems were increased with the decrease of the cooling water temperature. According to the results, the maximum cycle efficiency of KCS-11 yielded with at ammonia mass fraction of 92 % for 3000 kPa turbine inlet pressure of working fluid. The energy and exergy efficiencies of this system were determined as 10.2 % and 50.6 %, respectively. Singh and Kaushik (2013) parametrically examined the performance of exhaust gas powered KC. They reported that increasing the turbine inlet pressure increase the maximum cycle efficiency further corresponding to a much higher ammonia mass fraction and the best cycle performance is determined with the 80 % of ammonia mass fraction for the turbine inlet pressure of around 4000 kPa. Prananto et al. (2018) investigated the performance of KC which generates electrical power from the brine discharged from the geothermal fluid at the Wayang Windu geothermal power plant. They determined the power generation and energy efficiency of the system as 1600 kW and 13.2 %, respectively.

In this study, thermodynamic and economic analysis have been carried out to determine the optimum design parameters of the Kalina Cycle operating with a medium temperature geothermal resource. KSG-1 (Siemens' Kalina cycle system) Kalina Cycle is used for modeling of the system. The outlet temperature of the geothermal fluid from the evaporator, ammonia mass fraction, turbine inlet pressure and condenser pressure are variable parameters of the system. Geothermal energy Powered Kalina Cycle (GEPKC) is evaluated by using net present value (*NPV*) method from the economical point of view for different system designs. The investment costs of equipment of GEPKC are calculated by using Module Costing Technique. Also, the energy and exergy efficiencies of the GEPKC designs are calculated. The exergy destructions and the investment costs of the system equipment are determined.

GEOTHERMAL ENERGY POWERED KALINA CYCLE

The geothermal energy heat source temperature, cooling water temperature and thermodynamical properties of ammonia-water mixture are the design parameters of the GEPKC. In the GEPKC designs, the thermodynamical properties of the geothermal source in the Simav region are used (Arslan, 2008; Arslan, 2010; Arslan, 2011). The geothermal fluid is supplied from 9 wells. The temperature of the geothermal fluid is 406.65 K and its mass flow rate is 462 kg/s (Arslan, 2008; Arslan, 2010; Arslan, 2011). The vapor fraction of the geothermal fluid has been assumed as 10 %. GEPKC flow diagram is given in Figure 1.

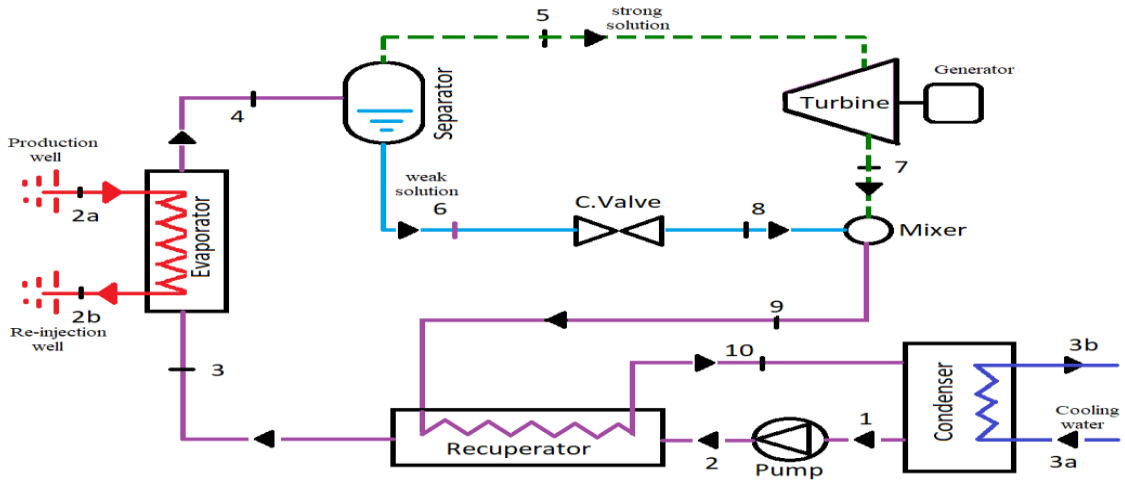

Figure 1. GEPKC flow diagram

.

As seen in Figure 1, the saturated liquid phased working fluid enters the pump (1) and outlets the pump (2) at evaporator pressure. The high-pressured working fluid enters the recuperator (3) and takes the heat of the mixer exhaust stream (9). The geothermal fluid (2a) is transferred the heat to the preheated working fluid (4) at the evaporator and re-injected to the well (2b). The working fluid is separated into two different flows at the separator. One is high ammonia concentration (strong solution) and vapor phased stream (5) and the other is low ammonia concentration (weak solution) and liquid phased stream (6). Superheated strong solution flow is expanded at the turbine (point 7) to produce power. At the same time, weak solution flows pass through the valve to expand the condenser pressure (8). And both weak solution and strong solution flows are mixed in the mixer and enters the recuperator (9). And it gives the heat to the high-pressured working fluid (2-3). The low-pressured ammonia-water mixture enters to the air-cooled condenser (10) and leaves as saturated liquid (1). The properties of the GEPKC equipment and parameters are given in Table 1.

Table 1. The properties of the GEPKC equipment and parameters (Arslan, 2010; Wang et al., 2017; Acar and Arslan, 2019).

Component	Parameter	Values
Geothermal fluid	Inlet temperature T_{2a}	406.65 K
	Outlet temperature T_{2b}	353.15 K, 363.15 K, 373.15 K
	Mass flow rate $\dot{m}_{2a}$	462 kg/s
Evaporator	Outlet temperature of mixture T_4	398.15 K
	Efficiency η_{eva}	0.85
Condenser	Inlet temperature T_{3a}	288.15 K
	Outlet temperature T_{3b}	298.15 K
	Pressure P_c	4 kPa
	Efficiency η_c	0.85
Generator	Efficiency η_g	0.95
Pump	Isentropic efficiency η_p	0.8
Recuperator	Efficiency η_r	0.85
Turbine	Isentropic efficiency η_{tr}	0.85

The GEPKC is designed for 90, 85, 80, 75, 70 % of ammonia mass fraction (α). The thermodynamic properties of the ammonia-water mixture are determined by Reference Fluid Thermodynamic and Transport Properties Database 10.1 (REFPROP) (Lemmon et al., 2018).

THERMODYNAMIC ANALYSIS

The governing energy equations of the GEPKC were obtained as follows. The heat transfer in the evaporator is calculated as;

$$\dot{Q}_{eva} = \dot{Q}_{gf} = \dot{m}_{gf} \cdot (h_{2a} - h_{2b}) = \left(\dot{m}_4 \cdot (h_4 - h_3)\right)/\eta_{eva} \quad (1)$$

The energy and mass equations of separator are given as;

$$\dot{m}_4 \cdot \alpha_4 = \dot{m}_5 \cdot \alpha_5 + \dot{m}_6 \cdot \alpha_6 \quad (2)$$

$$\dot{m}_4 = \dot{m}_5 + \dot{m}_6 \quad (3)$$

$$\dot{m}_4 \cdot h_4 = \dot{m}_5 \cdot h_5 + \dot{m}_6 \cdot h_6 \quad (4)$$

The turbine power output can be calculated as;

$$\dot{W}_{tr} = \dot{m}_5 \cdot (h_5 - h_7) = \dot{m}_5 \cdot (h_5 - h_{7s}) \cdot \eta_{tr} \quad (5)$$

Here, s indicates the isentropic process. The generator electric power can be calculated as;

$$\dot{W}_g = \eta_g \cdot \dot{W}_{tr} \quad (6)$$

The expansion through the control valve is an isenthalpic process.

$$h_6 = h_8 \quad (7)$$

The energy and mass equations of mixer are given as;

$$\dot{m}_9 \cdot \alpha_9 = \dot{m}_7 \cdot \alpha_7 + \dot{m}_8 \cdot \alpha_8 \quad (8)$$

$$\dot{m}_9 = \dot{m}_7 + \dot{m}_8 \quad (9)$$

$$\dot{m}_9 \cdot h_9 = \dot{m}_7 \cdot h_7 + \dot{m}_8 \cdot h_8 \quad (10)$$

The heat transfer in recuperator is given as;

$$\dot{Q}_r = \dot{m}_9 \cdot (h_9 - h_{10}) = \left(\dot{m}_2 \cdot (h_3 - h_2)\right)/\eta_r \quad (11)$$

The heat transfer in the condenser can be calculated by as;

$$\dot{Q}_c = \dot{m}_{10} \cdot (h_{10} - h_1) = \left(\dot{m}_{cw} \cdot (h_{3b} - h_{3a})\right)/\eta_c \quad (12)$$

The pump power input can be calculated as;

$$\dot{W}_p = \dot{m}_3 \cdot (h_3 - h_2) = \dot{m}_3 \cdot (h_{3s} - h_2)/\eta_p \quad (13)$$

The net power output of the GEPKC is;

$$\dot{W}_{net} = \dot{W}_g - \dot{W}_p \quad (14)$$

The energy efficiency of the GEPKC is calculated by;

$$\eta = \frac{\dot{W}_{net}}{\dot{Q}_{gf}} \quad (15)$$

The exergy balance equation for steady systems is:

$$\dot{E}_{X_{heat}} - \dot{E}_{X_{work}} + \dot{E}_{X_{m,i}} - \dot{E}_{X_{m,o}} = \dot{E}_{X_{dest}} \quad (16)$$

The exergy term of heat is calculated with;

$$\dot{E}_{X_{heat}} = \sum \left(1 - \frac{T_0}{T_e}\right) \cdot \dot{Q}_e \quad (17)$$

The exergy term of work is given as;

$$\dot{E}_{X_{work}} = \dot{W} \quad (18)$$

The mass flow exergy terms are given as;

$$\dot{E}_{X_{m,i}} = \sum \dot{m}_i \cdot \psi_i \quad (19)$$

$$\dot{E}_{X_{m,out}} = \sum \dot{m}_{out} \cdot \psi_{out} \quad (20)$$

where ψ; the physical and chemical exergy terms.

$$\psi = \psi_{ph} + \psi_{ch} \quad (21)$$

The physical exergy term is given as:

$$\psi_{ph} = (h - h_0) - T_0 \cdot (s - s_0) \quad (22)$$

where h is enthalpy, s is entropy, and the subscript zero indicates properties of fluids at the dead state. The reference state is 298.15 K and 101.325 kPa. The chemical exergy term given as;

$$\psi_{ch} = \frac{\alpha}{M_{NH_3}} \cdot e^0_{ch,NH_3} - \frac{(1-\alpha)}{M_{H_2O}} \cdot e^0_{ch,H_2O} \quad (23)$$

where $e^0_{ch,NH_3}$and e^0_{ch,H_2O} are molar exergy of the pure component at dead state conditions (kJ/mol), M is the molar mass (kg/mol), α is the mass ratio of ammonia in the mixture (Bejan et al., 1996).

The exergetic efficiency of system is then calculated by the following equation;

$$\varepsilon = 1 - \frac{\dot{E}_{X_{d,total}}}{\dot{E}_{X_{m,i}}} = \frac{\dot{W}_{net}}{(\dot{m}_{gf} \cdot (\psi_{2a} - \psi_{2b}))} \quad (24)$$

ECONOMIC ANALYSIS

The life cycle cost (C_{sys}) of GEPKC can be determined as;

$$C_{sys} = C_b - (C_{ic} + C_{sc} + C_{moc}) \quad (25)$$

where, C_{ic}; the investment costs (\$), C_{sc}; salvage cost (\$), C_{mc}; maintenance and operating costs (\$) and C_b; benefit (\$) of the GEPKC. The C_{sc} of GEPKC was taken as 10% of the C_{ic} (Acar and Arslan, 2017).

$$C_{sc} = C_{ic} \cdot 0.10 \quad (26)$$

The C_{mc} of GEPKC system was taken as 6 % of the C_{ic} of the GEPKC (Ashouri et al., 2015).

$$C_{moc} = C_{ic} \cdot 0.06 \quad (27)$$

The benefit of GEPKC includes electricity earning.

$$C_b = \dot{W}_{net} \cdot C_{elec} \cdot t_o \quad (28)$$

where C_{elec}; the unit price of electricity (\$/kWh) and t_o; operating time of plant is 8400 h per annum (Arslan, 2010). C_{elec} ic calculated by;

$$C_{elec} = \frac{CEPCI_{2018}}{CEPCI_{2014}} \cdot C_{elec,2014} \quad (29)$$

where $C_{elec,2014}$; the unit price of electricity in 2014 is 0.06 \$/kWh (Aminyavari et al., 2014), $CEPCI_{2018}$; Chemical Engineering Plant Cost Index in 2018 is 603.1 (CEPCI, 2018) and $CEPCI_{2014}$; Chemical Engineering Plant Cost Index in 2014 is 576.1 (Cao et al., 2018). The net cash flow;

$$C_{ncf} = (C_b - C_{moc}) \cdot (1 + i)^{t-1} \quad (30)$$

here, *i*; the interest rate and *t*; the related year time of cash flow. The *NPV* of GEPKC;

$$NPV = (C_{sc} - C_{ic}) + \sum_{t=0}^{ol} \frac{C_{ncf}}{(1+j)^t} \quad (31)$$

where *ol*; the lifetime of GEPKC, *j*; the discount rate. In this study, the lifetime of GEPKC system was added to calculations as 20 years. The discount and interest rates were taken as 18.5 % and 19.5 %, respectively (CBRT, 2019).

The investment cost of GEPKC is calculated by using Module Costing Technique (Cao et al., 2018; Turton et al., 2018). The data used to calculate the purchase cots of equipment were obtained from the literature in 2001 (Turton et al., 2018). The equipment costs were modified for the year 2018 by CEPCI. The equipment costs in 2018 can be calculated by;

$$C_{eq} = \frac{CEPCI_{2018}}{CEPCI_{2001}} \cdot F_{BM} \cdot C^0 \quad (32)$$

here, F_{BM}; the bare module cost factor, C^0; the purchase cost of equipment and $CEPCI_{2001}$;Chemical Engineering Plant Cost Index in 2001 is 397 (Cao at al., 2018). The purchase cost of equipment is calculated by (Turton et al., 2018);

$$log\, C^0 = K_1 + K_2 \cdot log\, X + K_3 \cdot (log X)^2 \quad (33)$$

here, *K*; constants are determined depending on the equipment and *X*; the parameter which is related to the equipment. These parameters are the total volume for separator, total heat transfer area for the evaporator,

Table 2. The constants of the cost equations (Turton et al., 2018).

Equipment	Constant										
	K_1	K_2	K_3	B_1	B_2	F_M	F_{BM}	F_P	c_1	c_2	C_3
Evaporator	4.6656	-0.1557	0.1547	0.9600	1.210	2.450	-	1.0000	0.0000	0.0000	0.0000
Separator	3.4974	0.4483	0.1074	2.2500	1.820	3.200	-	0.0000	0.0000	0.0000	0.0000
Recuperator	4.6656	-0.1557	0.1547	0.9600	1.210	2.450	-	1.0000	0.0000	0.0000	0.0000
Condenser	4.6420	0.3698	0.0025	-	-	-	3.000	0.0000	0.0000	0.0000	0.0000
Turbine	2.6259	1.4398	-0.1776	-	-	-	11.600	-	-	-	-
Pump	3.3892	0.0536	0.1538	1.8900	1.350	2.200	-	-	-0.3935	0.3957	-0.0023

condenser and recuperator, power consumption for pump and power output of the turbine.

The bare module cost factors can be calculated by (Turton et al., 2018);

$$F_{BM} = B_1 + B_2 \cdot F_M \cdot F_p \quad (34)$$

here, B; the constants based on equipment types, F_M; material factor and F_P; pressure factor. The pressure factor of the pump can be calculated by (Turton et al., 2018);

$$logF_P = C_1 + C_2 \cdot log\, P_p + C_3 \cdot \left(logP_p\right)^2 \quad (35)$$

here, P_p is the design pressure of the pump. The constants of the cost equations according to the equipment's are given in Table 2.

The heat transfer areas of the heat exchangers are calculated by using the logarithmic mean temperature difference (LMTD) method (Ashouri et al., 2015). Heat transfer coefficient (U) values of the equipment are given in Table 3.

Table 3. Heat transfer coefficient (U) values of the equipment (Ashouri et al., 2015; Rodríguez et al., 2013).

Equipment	U (W/m^2·K)
Recuperator	1000
Evaporator	900
Condenser	1100

The total volume of the separator can be calculated with (Cao at al., 2018; Zarrouka and Purnanto, 2015);

$$V_{sep} = \frac{\pi \cdot (3 \cdot D_{tube})^2}{4} \cdot (7 \cdot D_{tube} + 4 \cdot D_{tube}) \quad (36)$$

here D_{tube}; the diameter of the inlet pipe (m) and it is given by (Cao at al., 2018);

$$D_{tube} = \left(\frac{4 \cdot Q_{vs}/u_t}{\pi}\right)^{0.5} \quad (37)$$

here Q_{vs}; the volume flow rate of inlet flow of separator (m^3/s) and u_t; the terminal velocity of separator (m/s). The terminal velocity of vertical cyclone type separator is given by (Cao at al., 2018; Zarrouka and Purnanto, 2015);

$$u_t = Z \cdot \left(\frac{\rho_L - \rho_V}{\rho_V}\right)^{0.5} \quad (38)$$

Here ρ_L; liquid density (kg/m^3), ρ_V; vapor density (kg/m^3) and Z is 0.069 (Cao at al., 2018; Zarrouka and Purnanto, 2015).

The investment cost of the mixer is considered negligible.

RESULTS AND DISCUSSION

In this study, turbine inlet pressure, geothermal water outlet temperature at the evaporator, condenser pressure and ammonia mass fraction are the design and optimization parameters of GEPKC. 125 different GEPKC models are designed and energy efficiency, exergy efficiency and net present values of these models are calculated. The investment cost of each component is considered for economic investigation. Handling the operating parameters as P_4=4808 kPa and T_{2b}=353.15 K, the variation of energy efficiency of the GEPKC system with different ammonia mass fraction (α) and condenser pressure (P_{10}) obtained as seen in Fig. 2.

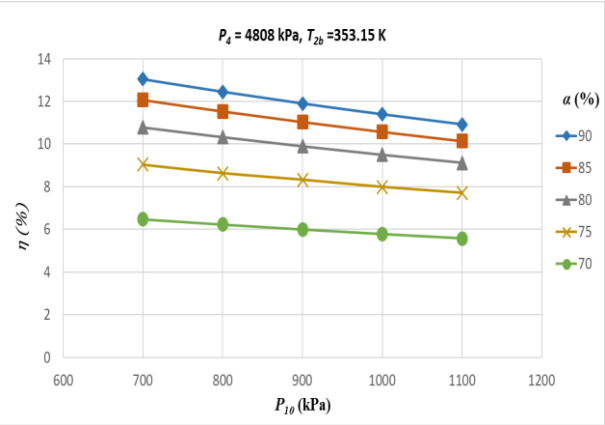

Figure 2. The variation of energy efficiency, η of GEPKC versus α and P_{10}.

According to Fig. 2, the η values of the GEPKC increase by the decrease of P_{10} and the increase of the ammonia mass fraction. The η values of the proposed system range between 5.57 % and 13.04 %. The highest η value of GEPKC system is obtained for 700 kPa of turbine outlet pressure and 90 % of ammonia mass fraction at 4808 kPa of turbine inlet pressure and 353.15 K of outlet temperature of the geothermal fluid from the evaporator. The η values of the system increase with the increase of the ammonia mass fraction and decrease of the condenser pressure. The change of exergy efficiency values of GEPKC system for P_4=4808 kPa and T_{1b}=353.15 K

according to different ammonia mass fraction (α) and turbine outlet pressure (P_{10}) are given in Fig. 3.

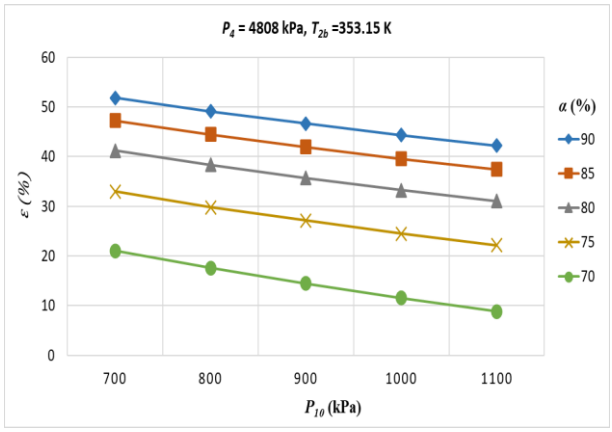

Figure 3. The variation of exergy efficiency, ε of GEPKC versus α and P_{10}.

According to Fig. 3, the ε values of the GEPKC increase by the decrease of P_{10} and the increase of the ammonia mass fraction. The ε values of the proposed system range between 8.79 % and 51.81 %. The highest ε value of GEPKC system is obtained for 700 kPa of turbine outlet pressure and 90 % of ammonia mass fraction at 4808 kPa of turbine inlet pressure and 353.15 K of outlet temperature of the geothermal fluid from the evaporator. The ε values of the system increase with the increase of the ammonia mass fraction and decrease of the condenser pressure. Handling the operating parameters as P_4=4808 kPa and T_{2b}=353.15 K, the variation of *NPV* of the GEPKC system with different ammonia mass fraction (α) and turbine outlet pressure (P_{10}) obtained as seen in Fig. 4.

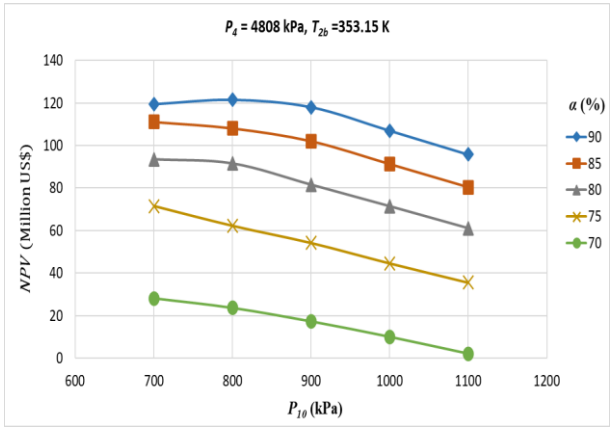

Figure 4. The variation of *NPV* of GEPKC versus α and P_{10}.

Fig. 4 shows that the *NPV* of the GEPKC decrease by the increase of P_{10} and the decrease of the ammonia mass fraction. The *NPV* of the proposed system range between 2.196 Million US$ and 121.446 Million US$. The maximum *NPV* of GEPKC system was obtained for 800 kPa of turbine outlet pressure and 90 % of ammonia mass fraction at 4808 kPa of turbine inlet pressure and 353.15 K of outlet temperature of the geothermal fluid from the evaporator. The change of the net power output values of GEPKC system for P_4=4808 kPa and T_{2b}=353.15 K according to different ammonia mass fraction (α) and turbine outlet pressure (P_{10}) are given in Fig. 5.

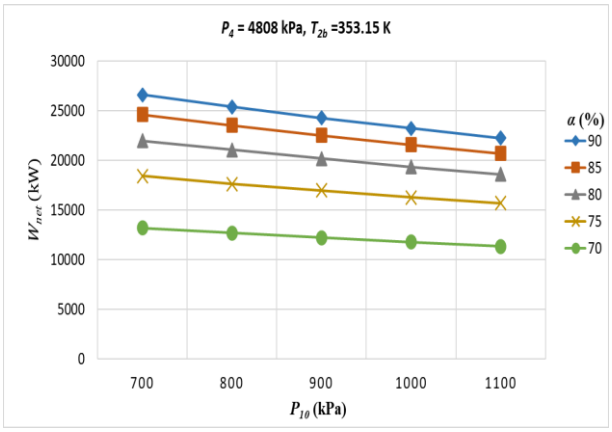

Figure 5. The variation of the net power output of GEPKC versus α and P_{10}.

According to Fig. 5, the net power output values of the GEPKC increase by the decrease of P_{10} and the increase of the ammonia mass fraction. The net power output values of the proposed system range between 11372.672 kW and 26633.930 kW. The highest net power output value of GEPKC system is obtained for 700 kPa of turbine outlet pressure and 90 % of ammonia mass fraction at 4808 kPa of turbine inlet pressure and 353.15 K of outlet temperature of the geothermal fluid from the evaporator. The net power output values of the system increase with the increase of the ammonia mass fraction and decrease of the condenser pressure. Handling the operating parameters as P_{10}=700 kPa and T_{2b}=353.15 K, the variation of energy efficiency of the GEPKC system with different ammonia mass fraction (α) and turbine inlet pressure (P_4) obtained as seen in Fig. 6.

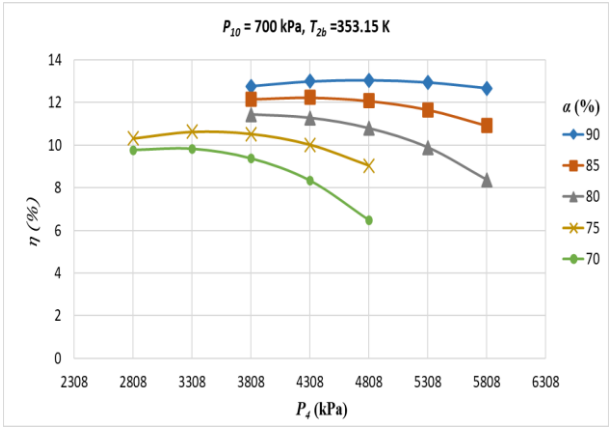

Figure 6. The variation of energy efficiency, η of GEPKC versus α and P_4.

According to Fig. 6, the η values of the proposed system range between 6.47 % and 13.04 %. The minimum η value of GEPKC system at the same ammonia mass fraction is obtained for the maximum value of turbine inlet pressure. Furthermore, the variation of the η values with the turbine inlet pressure for different ammonia mass fractions show different trends. The highest η value of GEPKC system is obtained for 4808 kPa of turbine

inlet pressure and 90 % of ammonia mass fraction at 700 kPa of turbine outlet pressure and 353.15 K of outlet temperature of the geothermal fluid from the evaporator. The change of ε values of GEPKC system for P_{10}=700 kPa and T_{2b}=353.15 K according to different ammonia mass fraction (α) and turbine inlet pressure (P_4) are given in Fig. 7.

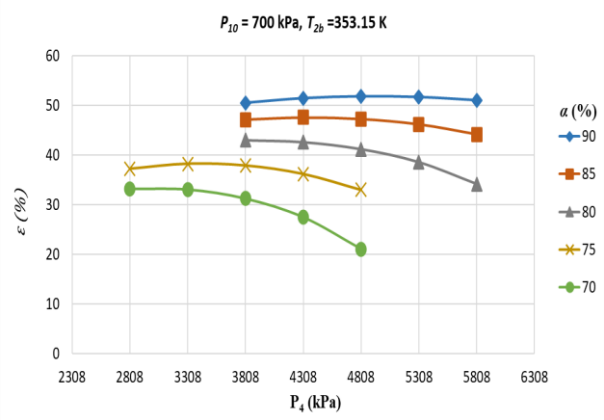

Figure 7. The variation of exergy efficiency, ε of GEPKC versus α and P_4.

According to Fig. 7, the ε values of the proposed system range between 21.01 % and 51.81 %. The maximum ε value of GEPKC system is obtained for 4808 kPa of turbine inlet pressure and 90 % of ammonia mass fraction at 700 kPa of turbine outlet pressure and 353.15 K of outlet temperature of the geothermal fluid from the evaporator. The change of *NPV* of GEPKC system for P_{10}=800 kPa and T_{2b}=353.15 K according to different ammonia mass fraction (α) and turbine inlet pressure (P_4) is given in Fig. 8.

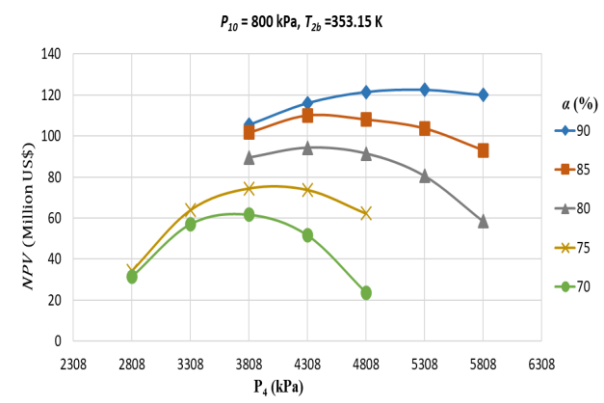

Figure 8. The variation of *NPV* of GEPKC versus α and P_4.

Fig. 8 shows that the *NPV* of the proposed system ranges between 23.656 Million US$ and 122.529 Million US$. The maximum *NPV* of GEPKC system is obtained for 800 kPa of turbine outlet pressure and 5308 kPa of turbine inlet pressure. For the same system, the energy and exergy efficiencies are calculated as 12.38 % and 46.71 %, respectively. The change of net power output values of GEPKC system for P_{10}=700 kPa and T_{2b}=353.15 K according to different ammonia mass fraction (α) and turbine inlet pressure (P_4) are given in Fig. 9.

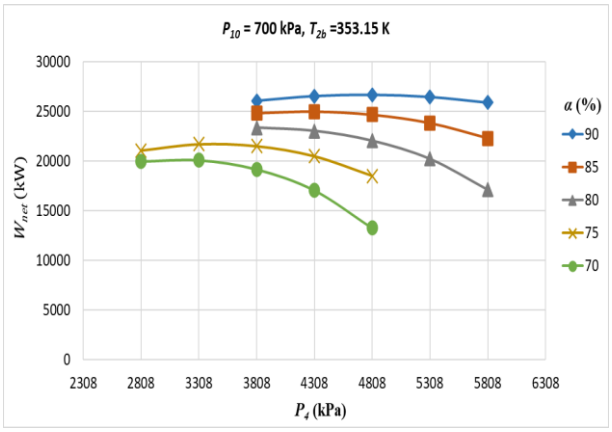

Figure 9. The variation of the net power output of GEPKC versus α and P_4.

According to Fig. 9, the variation of the net power output values of the GEPKC with the turbine inlet pressure for different ammonia mass fractions show the same trends. The net power output values of the proposed system range between 13218.33 kW and 26633.93 kW. The highest net power output value of GEPKC system is obtained as 26633.93 kW for 4808 kPa of turbine inlet pressure and 90 % of ammonia mass fraction at 700 kPa of turbine outlet pressure and 353.15 K of outlet temperature of the geothermal fluid from the evaporator. Handling the operating parameters as P_{10}=700 kPa and P_4=4808 kPa, the variation of ε of the GEPKC system with different outlet temperature of the geothermal fluid from the evaporator (T_{2b}) and ammonia mass fraction (α) obtained as seen in Fig. 10.

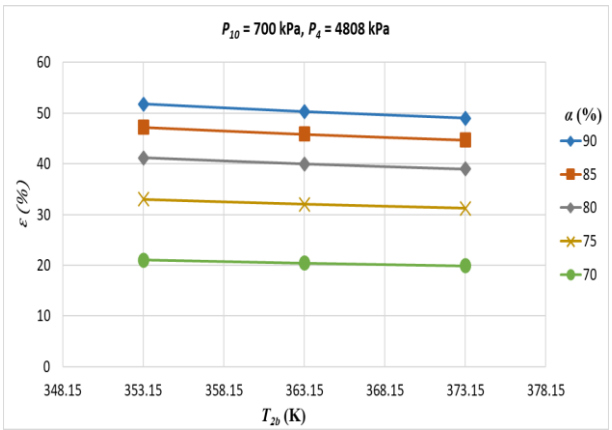

Figure 10. The variation of exergy efficiency, ε of GEPKC versus α and T_{2b}.

Fig. 10 shows that the ε values of the GEPKC increase by the decrease of outlet temperature of the geothermal fluid from the evaporator and the increase of the ammonia mass fraction. The ε values of the proposed system range between 19.88 % and 51.81 %. The highest exergy efficiency value of GEPKC system was obtained for 353.15 K of outlet temperature of the geothermal fluid from the evaporator. The ε values of the system increase with the increase of the ammonia mass fraction and outlet

temperature of the geothermal fluid from the evaporator. Handling the operating parameters as P_{10}=700 kPa and P_4=4808 kPa, the variation of *NPV* of the GEPKC system with different outlet temperature of the geothermal fluid from the evaporator (T_{2b}) and ammonia mass fraction (α) obtained as seen in Fig. 11.

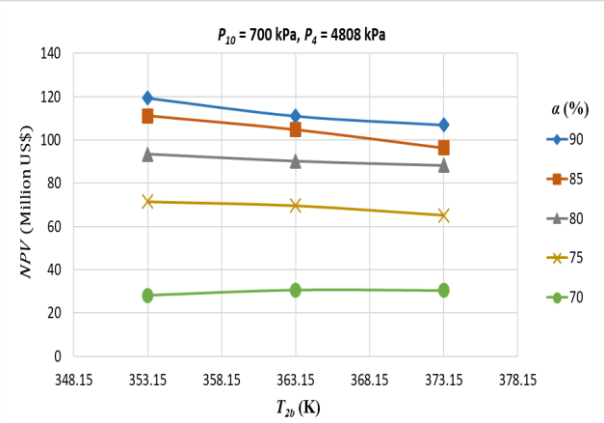

Figure 11. The variation of *NPV* of GEPKC versus α and T_{2b}.

Fig. 11 shows that the *NPV* of the GEPKC increase by the decrease of T_{2b} accepts 70 % of the ammonia mass fraction. The *NPV* of the proposed system ranges between 28.142 Million US$ and 119.377 Million US$. The maximum *NPV* of GEPKC was obtained for 353.15 K of the outlet temperature of the geothermal fluid from the evaporator and 90 % of the ammonia mass fraction. The change of net power output values of GEPKC for P_4=4808 kPa and P_{10}=700 kPa according to different ammonia mass fraction (α) and turbine outlet pressure (T_{2b}) are given in Fig. 12.

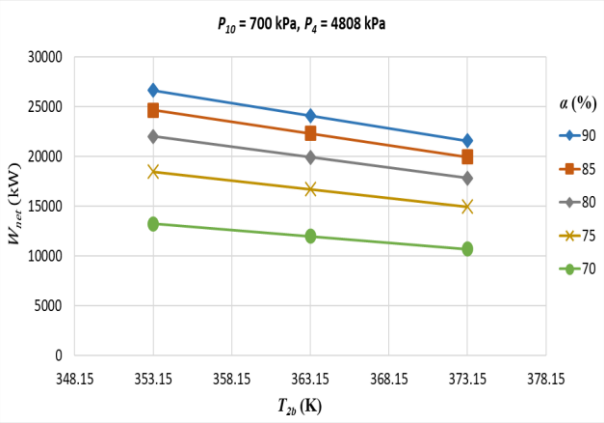

Figure 12. The variation of the net power output of GEPKC versus α and T_{2b}.

According to Fig. 12, the net power output values of the GEPKC increase by the decrease of T_{2b} and the increase of the ammonia mass fraction. The net power output values of the proposed system range between 10702.51 kW and 26633.93 kW. The net power output values of the system increase with the increase of the ammonia mass fraction and decrease of the outlet temperature of the geothermal fluid from the evaporator. Handling the operating parameters as P_4=4808 kPa, P_{10}=700 kPa and T_{2b}=353.15 K, the variation of exergy destructions of the system equipment with ammonia mass fraction are given in Fig. 13.

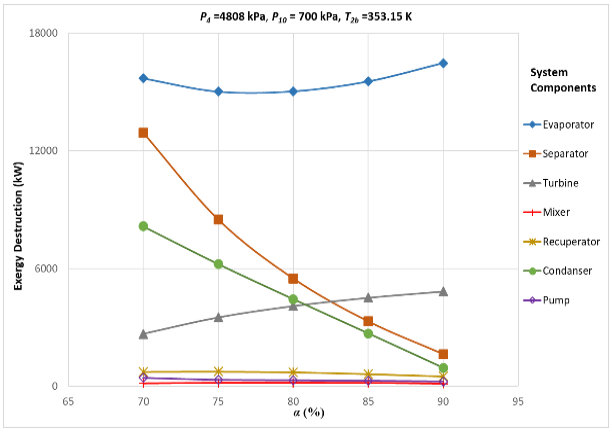

Figure 13. The variation of exergy destructions of system equipment versus α.

As seen in Fig. 13, the highest exergy destruction is determined as 16461.22 kW for the evaporator. The minimum exergy destruction in the evaporator is determined as 15010.84 kW at 75 % of ammonia mass fraction. The exergy destruction of separator and condenser decreases with the increase of the ammonia mass fraction. The exergy destruction of the turbine decreases with the decrease of the ammonia mass fraction. In the system design with 90 % ammonia mass fraction, the exergy destruction in the evaporator accounts for 66.5 % of the total exergy destruction in the system. The maximum exergy destruction occurs in the evaporator within the total exergy destruction of the system. Handling the operating parameters as P_4=4808 kPa, P_{10}=700 kPa and T_{2b}=353.15 K, the variation of investment costs of the system equipment with ammonia mass fraction are given in Fig. 14.

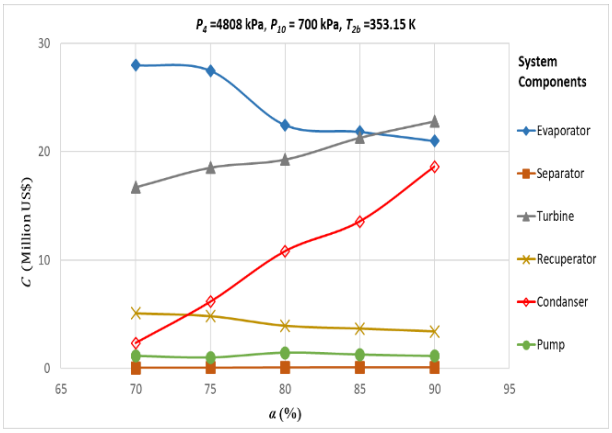

Figure 14. The variation of the investment cost of system equipment versus α.

As seen in Fig. 14, the highest investment cost is determined as 27.9927 Million US$ for the evaporator. The investment cost of the turbine, separator and condenser increase with the increase of the ammonia mass fraction. The investment costs of the evaporator and recuperator decrease with the increase of the ammonia mass fraction. According to the energy efficiency and

Table 4. The optimum GEPKC design parameters.

	T (K)	P (kPa)	h (kJ/kg)	s (kJ/kg·K)	$\dot{m}$ (kg/s)	α (%)	E_x^{ch} (kW)	Ψ (kJ/kg)
1	290.60	700	358.04	1.6851	151.94	90	2714097.31	196.66
2	291.72	4808	365.91	1.6905	151.94	90	2714097.31	202.92
3	309.93	4808	449.89	1.9697	151.94	90	2714097.31	203.65
4	398.15	4808	1592.10	5.0858	151.94	90	2714097.31	416.80
5	398.15	4808	1789.10	5.6081	123.68	96.416	2366346.95	458.08
6	398.15	4808	729.96	2.7998	28.25	61.914	347650.36	178.31
7	308.37	700	1561.81	5.7391	123.68	96.416	2366346.95	191.73
8	323.04	700	729.96	2.9558	28.25	61.914	347650.36	189.72
9	314.93	700	1407.12	5.2243	151.93	90	2714097.31	190.53
10	307.21	700	1308.32	4.9065	151.93	90	2714097.31	186.48
2a	406.65	300	777.13	2.2030	462.00	-		461.33
2b	353.15	300	335.21	1.0754	462.00	-		355.61
3a	288.15	4	62.98	0.2244	3450.31	-		728.59
3b	298.15	4	104.83	0.3672	3450.31	-		727.87
$\dot{W}_{net}$	26633.93 kW							
η	13.04 %							
ε	51.81 %							
NPV	119.377 Million US$							

exergy efficiency values of GEPKC, the optimum plant design parameters are given in Table 4.

As seen in Table 4, the *NPV*, energy and exergy efficiency of the most effective GEPKC are determined as 119.377 Million US$, 13.04 % and 51.81 %, respectively. The geothermal water outlet temperature at the evaporator, ammonia mass fraction, turbine inlet pressure and condenser pressure of this system are determined as 353.15 K, 90 %, 4808 kPa and 700 kPa, respectively.

The thermodynamic model of GEPKC is validated comparing the results obtained with published literature results (Arslan, 2010; Wang et al., 2017), as shown in Table 5 and Table 6. The data obtained from Arslan (2010) are used to validate the thermodynamic model according to the thermodynamic properties of geothermal source and cooling water.

As seen in Table 5, the energy efficiency of the KCS-34 system, which has the same geothermal resource characteristics, is 2.5% higher than that of the KCS-1 system. When both systems are evaluated in terms of exergy efficiency, it is seen that the KCS-1 system is 12.6% more efficient than the KCS-34 system. The thermodynamic properties of the key state points well coincide with each other.

Table 5. Model validation with the results of Arslan (2017).

Parameter	**Arslan (2010)**	**Present study**
Cycle type	KCS-34	KC-1
Mass flow rate of geothermal fluid	462 kg/s	462 kg/s
Geothermal fluid inlet temperature (evaporator)	406.65 K	406.65 K
Geothermal fluid outlet temperature (evaporator)	353.15 K	353.15 K
Working fluid ammonia mass fraction	90 %	90 %
Turbine inlet ammonia mass fraction of working fluid	93 %	93.70 %
Turbine inlet temperature of working fluid	403 K	398.15 K
Turbine inlet pressure of working fluid	3000 kPa	3308 kPa
Condensing temperature	311.85 K	312.43 K
Condensing pressure	714 kPa	700 kPa
Cooling water inlet temperature (condenser)	288.15 K	288.15 K
Cooling water outlet temperature (condenser)	298.15 K	298.15 K
Mass flow rate of cooling water	3463.6	3110 kg/s
η	14.8 %	12.3 %
ε	36.2 %	48.8 %

Table 6. Model validation with the results of Wang et al. (2017).

State	Present study				Wang et al. (2017)			
	***T* (K)**	***P* (kPa)**	***ṁ* (kg/s)**	***α* (%)**	***T* (K)**	***P* (kPa)**	***ṁ* (kg/s)**	***α* (%)**
1	298.79	700	177.06	0.750	282.35	435	32.673	0.760
2	299.28	2808	177.06	0.750	282.71	2392	32.673	0.760
3	338.20	2808	177.06	0.750	321.77	2325	32.673	0.760
4	398.15	2808	177.06	0.750	380.45	2280	32.67	0.760
5	398.15	2808	113.39	0.921	380.45	2280	19.914	0.964
6	398.15	2808	58.77	0.405	380.45	2280	12.759	0.441
7	341.11	700	113.39	0.921	312.95	447	19.914	0.964
8	345.36	700	58.77	0.405	334.76	447	12.759	0.441
9	343.20	700	177.06	0.750	326.77	447	32.673	0.760
10	327.31	700	177.06	0.750	308.29	443	32.673	0.760
2a	406.65	300	462	*gf*	393.15	2000	142	*gf*
2b	353.15	300	462	*gf*	341.78	1961	142	*gf*
3a	288.15	4	3507	*water*	271.85	118	2259	*air*
3b	298.15	4	3507	*water*	283.60	113	2259	*air*
η	10.30 %				10.48 %			
ε	37.22 %				48.10 %			

As seen in Table 6, the energy efficiency value in Reference (Wang et al., 2017) is 0.18 % higher than the present work. The exergy efficiency of the system in Reference (Wang et al., 2017) is 18 % higher than the exergy efficiency of the GEPKC. The reason of this difference is that the temperature and mass flow rate of the resource is used in this study are higher than the Reference (Wang et al., 2017). Considering the properties of the geothermal resources used in the studies, it is seen that the thermodynamic properties of the state points coincide with each other. It is observed that especially the pressure values and the ammonia mass fractions of the state points are compatible with the Reference (Wang et al., 2017).

CONCLUSION

In this study, the GEPKC is designed for different geothermal water outlet temperature at evaporator, ammonia mass fraction, turbine inlet pressure and condenser pressure. The net power output, *NPV*, energy and exergy efficiencies of the GEPKC are determined. The most effective system parameters determined as P_{10}=700 kPa, P_4=4808 kPa, T_{2b}=353.15 K and α=90 % according to the energy and exergy efficiencies. The energy and exergy efficiencies of this system are determined as 13.04 % and 51.81 %, respectively. In addition, the *NPV* value of this system is calculated as 119.377 Million US$ and it is seen that it is suitable for investment in economic terms. The net power output of this system is calculated as 26633.93 kW. Also, the following results were obtained:

- The net power output, energy and exergy efficiencies of the GEPKC increase with the decrease of the condenser pressure.
- The investment cost of the evaporator is found to have a significant effect on the NPV value. The investment cost of the evaporator decreases with the increase of the ammonia mass fraction.
- The maximum exergy destruction is realized in the evaporator.
- The exergy efficiency values of the GEPKC increase by the decrease of outlet temperature of the geothermal fluid from the evaporator, turbine outlet pressure and the increase of the ammonia mass fraction.
- The *NPV* of the GEPKC increases with the increase of ammonia mass fraction ratio.

REFERENCES

Acar, S.M. and Arslan, O., 2017, Exergo-economic evaluation of a new drying system boosted by Ranque–Hilsch vortex tube, *Applied Thermal Engineering*, 124, 1–16.

Acar, S.M. and Arslan, O., 2019, Energy and exergy analysis of solar energy-integrated, geothermal energy-powered Organic Rankine Cycle, *Journal of Thermal Analysis and Calorimetry*, 137 (2), 659-666.

Aminyavari, M., Najafi, B., Shirazi, A., and Rinaldi, F., 2014, Exergetic, economic and environmental (3E) analyses, and multi objective optimization of a CO_2/NH_3 cascade refrigeration system, *Applied Thermal Engineering*, 65, 42-50.

Arslan, O., 2008, *Ultimate evaluation of Simav-Eynal geothermal resources: design of integrated system and its energy-exergy analysis*, Ph.D. thesis, Institute of Applied Sciences Eskisehir Osmangazi University, Turkey (in Turkish).

Arslan, O., 2010, Exergoeconomic evaluation of electricity generation by the medium temperature geothermal resources, using a Kalina cycle: Simav case study, *International Journal of Thermal Sciences*, 49 (9), 1866-1873.

Arslan, O., 2011, Power generation from medium temperature geothermal resources: ANN-based optimization of Kalina cycle system-34, *Energy*, 36 (5), 2528-2534.

Ashouri, M., Vandani, A.M.K., Mehrpooya, M., Ahmadi, M.H. and Abdollahpour, A., 2015, Techno-economic assessment of Kalina cycle driven by a parabolic trough solar collector, *Energy Conversion and Management*, 105, 1328-1339.

Bejan, A., Tsatsaronis, G. and Moran, M., 1996, Thermal design and optimization, New York: John Wiley & Sons Inc., USA.

Cao, L., Wang, J., Chen, L. and Dai, Y., 2018, Comprehensive analysis and optimization of Kalina-Flash cycles for low-grade heat source, *Applied Thermal Engineering*, 131, 540-552.

Deepak, K., Gupta, A.V.S.S.K.S., Srinivas, T., Prabhakar Vattikuti, S.V. and Deva Prasasd, S., 2014, Investigation of separator parameters in Kalina Cycle systems, *International Journal of Current Engineering and Technology*, Special Issue 2, 496-500.

Eller, T., Herberle, F. and Brüggemann, D., 2017, Techno-economic analysis of novel working fluid pairs for the Kalina cycle, *Energy Procedia*, 129, 113-120.

He, J., Chao, L., Xu, X., Li, Y., Wu, S. and Xu, J., 2014, Performance research on modified KCS (Kalina cycle system) 11without throttle valve, *Energy*, 64, 389-397.

Igobo, O.N. and Davies, P.A., 2016, Review of low-temperature vapour power cycle engines with quasi-isothermal expansion, *Applied Energy*, 180, 834-848.

Internet, 2019, CEPCI Chemical Engineering Plant Cost Index, Plant Cost Index 2018, https://www.chemengonline.com/2019-cepci-updates-january-prelim-and-december-2018-final/.

Internet, 2019, CBRT Central Bank of Republic of Turkish, *Discount rate and interest rate of Turkey 2018*, https://www.tcmb.gov.tr/wps/wcm/connect/TR/TCMB+TR/Main+Menu/Temel+Faaliyetler/Para+Politikasi/Reeskont+ve+Avans+Faiz+Oranlari.

Kalina, A.I., 1984, Combined-Cycle System with Novel Bottoming Cycle, *Journal of Engineering for Gas Turbines and Power*, 106 (4), 737-742.

Lemmon, E.W., Bell, I.H., Huber, M.L. and McLinden, M.O., 2018, *NIST Standard Reference Database 23: Reference Fluid Thermodynamic and Transport Properties-REFPROP*, Version 10.0, National Institute of Standards and Technology.

Li, X., Zhang, Q. and Li, X., 2013, A Kalina cycle with ejector, *Energy*, 54, 212-219.

Mergner, H. and Weimer, T., 2015, Performance of ammonia-water based cycles for power generation from low enthalpy heat sources. *Energy*, 88, 93-100.

Modi, A. and Haglind, F., 2015, Thermodynamic optimisation and analysis of four Kalina cycle layouts for high temperature applications, *Applied Thermal Engineering*, 76, 196-205.

Nasruddin, Usvika R., Rifaldi, M. and Noor, A., 2009, Energy and exergy analysis of Kalina cycle system (KCS) 34 with mass fraction ammonia-water mixture variation, *Journal of Mechanical Science and Technology*, 23, 1871-1876.

Prananto, L.A., Zaini, I.N., Mahendranata, B.I., Juangsa, F.B., Aziz, M. and Soelaiman, T.A.F., 2018, Use of the Kalina cycle as a bottoming cycle in a geothermal power plant: casestudy of the Wayang Windu geothermal power plant, *Applied Thermal Engineering*,132, 686-696.

Rodríguez, C.E.C., Palacio, J.C.E., Venturini, O.J., Lora, E.E.S., Cobas, V.M., dos Santos, D.M., Dotto F.R.L. and Gialluca, V., 2013, Exergetic and economic comparison of ORC and Kalina cycle for low temperature enhanced geothermal system in Brazil, *Applied Thermal Engineering*, 52 (1), 109-119.

Sadeghi, S., Saffari, H. and Bahadormanesh, N., 2015, Optimization of a modified double-turbine Kalina cycle by using Artificial Bee Colony algorithm, *Applied Thermal Engineering*, 91, 19-32.

Saffari, H., Sadeghi, S., Khoshzat, M. and Mehregan, P., 2016, Thermodynamic analysis and optimization of a geothermal Kalina cycle system using Artificial Bee Colony algorithm, *Renewable Energy*, 89, 154-167.

Singh, O.K. and Kaushik, S.C., 2013, Energy and exergy analysis and optimization of Kalina cycle coupled with a coalfired steam power plant, *Applied Thermal Engineering*, 51, 787-800.

Sun, F., Zhou, W., Ikegami, Y., Nakagami, H. and Su, X., 2014, Energy-exergy analysis and optimization of the solar-boosted Kalina cycle system 11 (KCS-11), *Renewable Energy*, 66, 268-279.

Turton, R., Shaeiwitz, J.A., Bhattacharyya, D. and Whiting, WB., 2018, *Analysis, Synthesis, and Design of Chemical Processes*. 5th ed, Upper Saddle River New Jersey: Prentice Hall, USA.

Varma, G.V.P. and Srinivas, T., 2017, Power generation from low temperature heat recovery, *Energy Conversion and Management*, 151, 123-135.

Wang, E. and Yu, Z., 2016, A numerical analysis of a composition-adjustable Kalina cycle power plant for power generation from low-temperature geothermal heat sources, *Applied Energy*, 180, 834-848.

Wang, E., Yu, Z. and Zhang, F., 2017, Investigation on efficiency improvement of a Kalina cycle by sliding condensation pressure method, *Energy Conversion and Management*, 151, 123-135.

Yari, M., Mehr, A.S., Zare, V., Mahmoudi, S.M.S. and Rosen, M.A., 2015, Exergoeconomic comparison of TLC (trilateral Rankine cycle), ORC (organic Rankine cycle) and Kalina cycle using a lowgrade heat source, *Energy*, 83, 712-722.

Zare, V. and Moalemian, A., 2017, Parabolic trough solar collectors integrated with a Kalina cycle for high temperature applications: Energy, exergy and economic analyses, *Energy Conversion and Management*, 151, 681-692.

Zarrouka, S.J. and Purnanto, M.H., 2015, Geothermal steam-water separators; design overview, *Geothermics*, 53, 236-254.

Zhang, X., He, M. and Zhang, Y., 2012, A review of research on the Kalina cycle. *Renewable Sustainable Energy Reviews*, 16, 5309-5318.